Physica C: Superconductivity and its applications 520 (2016) 24–32

Contents lists available at ScienceDirect

Physica C: Superconductivity and its applications

journal homepage: www.elsevier.com/locate/physc

Spin-wave theory of two-magnon Raman scattering in iron Pnictides and Chalcogenides

C.S. Liu*

Department of Physics, Yanshan University, Qinhuangdao 006004, China

ARTICLE INFO

Article history:
Received 6 June 2015
Revised 19 October 2015
Accepted 18 November 2015
Available online 2 December 2015

Keywords:
Two-magnon Raman scattering
Iron-based superconductor
Linear spin wave approximation
Optical magnon
Acoustic magnon

ABSTRACT

Motivated by the experimental measurement of the two-magnon Raman scattering in iron Pnictides and Chalcogenides superconductors (Okazaki et al., 2011; Sugai et al., 2012), the underlying spin excitations of the $(\pi, 0)$ collinear and the $(\pi/2, \pi/2)$ diagonal double stripe antiferromagnetic superstructures are investigated in detail with the spin density wave approximation. By calculating the Fleury–London (FL) Raman cross-section of various quantum spin models proposed for this new class of superconductors, it is found that the unfrustrated quantum spin models are well consistent with the Raman data. Our calculation results also show that the broad peak around 2500 cm^{-1} of iron Pnictides in B_g channel come from the quasiparticle excitations of two optical magnons, whereas, in A_g channel the Raman response is from two optical magnons and two acoustic magnons with almost the same weights. In addition, our calculation results reveal that the broad peak around 2300 cm^{-1} of the iron Chalcogenides in B_g channel is caused by one acoustic magnon and one optical magnon, which is simultaneously excited by the Raman scattering. While in A_g channel, Raman scattering will mainly excite two optical magnons.

1. Introduction

In recent years, superconductivity has been observed in several classes of iron-based materials [1]. These quasi-two dimensional materials with a layered structure exhibit antiferromagnetic (AF) order in the parent phases. Their superconductivity emerges by suppressing magnetism (substituting the element) or pressurizing the material as in the high-T_c cuprate superconductors. However, the parent compounds of these classes of superconductors are multiorbital systems and remain metallic even in the AF state. In contrast, the parent material of the cuprates is a Mott insulator and can be described by an effective single-band model. In order to understand the origin of their superconductivity, it is necessary to study the magnetism in this new class of superconductors.

Two theories are presented to reveal the origin of the magnetism in iron-based superconductor. One theory is based on the Fermi surface nesting between the electron and hole pockets at the zone corner and center, respectively [2]. On the contrary, the As-bridged AF superexchange interaction was also considered as the driving force for the local interactions [3–5]. Although there are the contradictory evidences regarding the microscopic origin of the AF order, some local moment models have been widely used to explain the magnetic properties of iron-based superconductor.

A brief summary of various quantum spin models proposed for this new class of superconductors is in order here. The iron-based superconductors can be generally divided into two chemical classes, i.e., the iron Pnictides and iron Chalcogenides. In the iron Pnictides, two theories based on the localized moments have been proposed to explain the collinear AF phase [2,4–8]. One theory is the spatially anisotropic J_{1a}–J_{1b}–J_2 model, where the coupling is ferromagnetic (FM) in one direction and AF in the other. The other theory is the strongly frustrated J_1–J_2 model. Similarly, the diagonal double stripe AF order in iron Chalcogenides can be obtained either by invoking strong frustration in a J_1–J_2–J_3 model [9] or from a picture of correlated local moments with orbital degeneracy, coupled with a small density of itinerant electrons [10]. These models vary greatly in the degree of magnetic frustration.

In order to understand the origin of the AF order, it is necessary to determine the coupling parameters in different family of the iron-based superconductors. Among all magnetic measurement approaches, inelastic neutron scattering and polarized light Raman Scattering are two important methods to detect the spin excitations. Raman scattering is related to four-operator terms with the inherent momentum constraints. The largest contribution comes from two-magnon excitations [11]. Neutron scattering measurement is related to two operator terms which can in principle access to

* Tel.: +8613933533157.
E-mail address: csliu@ysu.edu.cn

http://dx.doi.org/10.1016/j.physc.2015.11.005
0921-4534/

the full wave vector. When the spin correlations transverse to the ordered spin direction z, one-magnon events will occur. However, the finite spin reduction allows for the presence of longitudinal fluctuations. The event can be described in terms of two-magnon scattering [12,13]. The above two measurements are considered as the basic and the complementary methods to detect the spin excitations in an AF system. In particular, the magnetic Raman scattering detects short-wavelength spin fluctuations, which can serve as an independent measure of the underlying spin interactions. The well-defined peak of two-magnon processes at energy $\omega \approx 3J\,(s = 1/2)$ in square-lattice antiferromagnetic structures [14,15] has been widely explored in cuprate superconductors.

The inelastic neutron scattering experiments have been used to map spin-wave excitations in the Pnictides, such as $CaFe_2As_2$ [16,17], $BaFe_2As_2$ [18,19] and $SrFe_2As_2$ [20,21] , as well as in iron Chalcogenides $Fe_{1+y}Te$ [22,23]. The exchange interacting parameters are obtained by fitting the spin wave dispersion with the short-range superexchange interaction and the total energy of long-range AF stripe spin structure. However, it is found that the exchange interaction energies vary greatly between the two models [16,19]. Raman scattering by magnetic excitations was also performed on high-quality single crystals of $BaFe_2As_2$ [24] and $Fe_{1+y}Te_{1-x}Se_x$ [25] superconductors. The broad peaks are found around 2500 cm^{-1} and 2300 cm^{-1}, respectively. It is naturally expected that Raman scattering data can provide more important spin-related information, such as exchange coupling constant, evolution of spin order with magnetic fields or temperatures, etc.

The two-magnon Raman spectra are calculated for various spin models proposed for the iron-based superconductors with exact diagonalization method [26]. The calculation results show that the two-magnon Raman responses are sensitive to the level of magnetic frustration. The numerical results indicate that the Pnictides and Chalcogenides favor spatially anisotropic models and the amount of magnetic frustration is small. However, the exact diagonalization in a small cluster will inevitably result in the finite-size effects although it gives small corrections to the Raman resonance energy.

In this paper, following the Fleury–Loudon (FL) formalism [11], I investigate the two-magnon Raman spectra for strongly frustrated models and spatially anisotropic models that are unfrustrated. Using spin-wave theory, I calculate two-magnon Raman cross-section and compare it to the Raman spectra for the iron Pnictides and Chalcogenides. This method, in particular, enables us to understand in detail the directional dependence of quasiparticle excitations in the Brillouin zone. This is the goal of the present paper. The main contributions of this paper are summarized as follows:

1. The weights of quasiparticle excitation relating to the two energy branches are given in the two-magnon Raman response.
2. The $(\pi/2, 0)$ collinear AF order in iron Pnictides should contain two energy branches instead of one branch, which needs to be detected further.
3. For the iron Chalcogenides, the exchange interaction parameters should be re-studied, since obvious differences exist between two-magnon Raman scattering, the first principles calculations and the inelastic neutron scattering.

The paper is organized as the following. In Section 2, I give the quantum spin Hamiltonian for iron Pnictides and Chalcogenides superconductors. Using the standard spin wave approximation, the model Hamiltonian is diagonalized in Section 2.1, the FL Raman scattering operators are then presented in Section 2.2. With the Kubo formulae in linear response theory, symmetry-channel dependent irreducible Raman response function is derived in Section 2.3. Raman responses are calculated and compared with experimental data in Section 3.1 for iron Pnictides and Section 3.2 for iron Chalcogenides respectively. Section 4 is a summary of this paper.

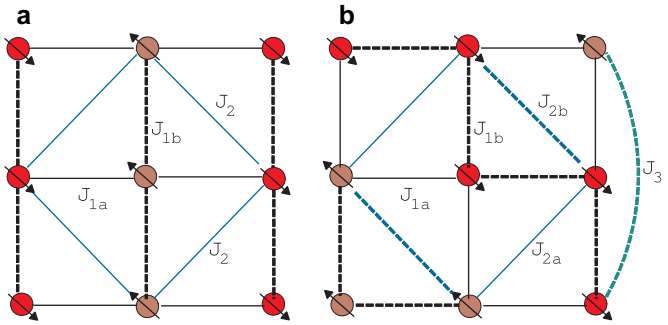

Fig. 1. (a) Schematic representation of in-plane Fe square lattice for (a) the $(\pi, 0)$ collinear AF order in iron Pnictides, and (b) the $(\pi/2, \pi/2)$ diagonal double stripe AF order in iron Chalcogenides. The magnetic exchange parameters $J_{1a}, J_{1b}, J_{2a}, J_{2b}$ and J_3 are shown in Table 1.

2. Theory

2.1. Model Hamiltonian

I start with the quantum spin model

$$H = \sum_{ij} \frac{J_{ij}}{2} \mathbf{S}_i \cdot \mathbf{S}_j \tag{1}$$

on a square lattice with up to third nearest-neighbor exchange J_{ij} to understand the magnetic excitation in iron Pnictides and Chalcogenides. Depending on the interaction parameters J_{ij}, the model can support ground states of different broken symmetries, such as the $(\pi, 0)$ collinear AF order [see Fig. 1(a)] and the $(\pi/2, \pi/2)$ diagonal double stripe order [see Fig. 1(b)]. To solve the Hamiltonian in Eq. (1), one can use standard linear spin wave approximation.

The dispersion relations of the collinear AF superstructure are given by [16,27]: $E_{\mathbf{k}} = \sqrt{A_{\mathbf{k}}^2 - B_{\mathbf{k}}^2}$, where

$$\begin{aligned} A_{\mathbf{k}} &= 2S[J_{1b}(\cos(k_x) - 1) + J_{1a} + 2J_2 + J_z], \\ B_{\mathbf{k}} &= -2S[J_{1a}\cos(k_y) + 2J_2\cos(k_x)\cos(k_y)]. \end{aligned} \tag{2}$$

Here J_z is the out-of-plane exchange interactions.

In addition, the spin lattices are generally divided into two sublattices to bosonize the Hamiltonian (1) [9,23]. A generic position of the spin shown in Fig. (1) is given by $\mathbf{r} = m\mathbf{l_1} + n\mathbf{l_2}$, where m, n are integers. $\mathbf{l_1}$ and $\mathbf{l_2}$ are unit vectors in the lattice x–y space. The linear spin wave approximation of the operators is then given by: for $m + n =$ odd:

$$\begin{aligned} S^+_{m,n} &= \sqrt{2S}c_{m,n}, \\ S^-_{m,n} &= \sqrt{2S}c^\dagger_{m,n}, \\ S^z_{m,n} &= S - c^\dagger_{m,n}c_{m,n}; \end{aligned} \tag{3}$$

for $m + n =$ even:

$$\begin{aligned} S^+_{m,n} &= \sqrt{2S}d_{m,n}, \\ S^-_{m,n} &= \sqrt{2S}d^\dagger_{m,n}, \\ S^z_{m,n} &= S - d^\dagger_{m,n}d_{m,n}. \end{aligned} \tag{4}$$

Define $\psi^\dagger_{\mathbf{k}} = (c^\dagger_{\mathbf{k}}, d^\dagger_{\mathbf{k}}, c_{-\mathbf{k}}, d_{-\mathbf{k}})$ and we have

$$H = \frac{1}{2}\sum_{\mathbf{k}} \psi^\dagger_{\mathbf{k}} \begin{pmatrix} A & D & B & C \\ D & A & C & B \\ B & C & A & D \\ C & B & D & A \end{pmatrix} \psi^\dagger_{\mathbf{k}}. \tag{5}$$